Int. J. Adv. Appl. Math. and Mech. 12(4) (2025) pages 102–119 (ISSN: 2347-2529)
Journal homepage: www.ijaamm.com

International Journal of Advances in Applied Mathematics and Mechanics

# Study and Numerical Resolution of a Temperature Control Problem in a Climate Model

**Research Article**

**TAHIROU ABOUBACAR Haboubacar[1], DJIBO Moustapha[2,*] TRAORE Aboubakari[3], Pr SALEY Bisso[1]**

[1] *Department of Mathematics and Informatic, Abdou Moumouni Unversity, Niamey, NIGER*
[2] *Department of Fundamentals Sciences, Dosso Unversity, Dosso, NIGER*
[3] *Higher Normal School of Abidjan, Côte d'Ivoire*

**Volume 12, Issue 04**
**Received:** 22 February 2025
**Accepted (in revised version):** 25 March 2025

**Abstract:** This work aims to study the null controllability of a simplified climate model where control acts to modify the albedo of a specific region on the Earth's surface. A mathematical analysis is conducted, followed by a numerical resolution coupling the spectral method and Adomian's decomposition method.

**MSC:** 49N05 • 80M50 • 93C05 • 93C20

**Keywords:** Albedo • Climate • Null controllability • Observability inequality • Carleman inequality • Spectral method • Adomian decomposition method • Latitude



## 1. Introduction

The pollution of our planet is caused by certain human activities. Climate change is one of the consequences of this pollution. It results in an increase in surface temperature on Earth, as well as an intensification of natural disasters and their magnitude.

The effects of climate change are numerous. The consequences of such disruptions are economic, environmental, and social. Hence, it is necessary to take action to mitigate the harmful effects of this phenomenon. Given the complexity of the phenomenon, a theoretical study is necessary beforehand to make better-informed decisions. Mathematical tools are the most suitable for contributing to this study. One of the mathematical models representing this phenomenon is a simplified climate model (see [10, 29, 32, 33, 37, 41, 45, 49, 51, 55]). Thus, we study the null controllability of this model through a possible modification of the albedo to control the temperature in a specific region of the Earth's surface [29, 37]. This study is accompanied by a numerical simulation based on a linear coupling approach of the spectral method and Adomian's decomposition method [23, 35].

* Corresponding author.
*E-mail address(es):* tahirouaa9393@gmail.com (TAHIROU ABOUBACAR Haboubacar), moustaphad530@gmail.com (DJIBO Moustapha), traoreabou08@gmail.com (TRAORE Aboubakari), bsaley@yahoo.fr (Pr SALEY Bisso).

## 2. Model Problem

Let $T > 0$ be a given time, $\Omega$ a bounded and regular open subset of $\mathbb{R}^n$, $\omega$ a subset of $\Omega$, and $\mathbf{1}_\omega$ the indicator function. We define $\Lambda = ]0, T[\times\Omega$. We will study the model as a local control problem with a Dirichlet boundary condition:

$$\begin{cases} \dfrac{\partial y}{\partial t} - \Delta y + A + By = QS(x^0)[1-\alpha(x^0)\mathbf{1}_\omega u] & \forall (t,x) \in ]0,T[\times\Omega \\ y(0,x) = y_0(x) & \forall x \in \Omega \\ y(t,x) = 0 & \forall (t,x) \in ]0,T[\times\partial\Omega. \end{cases} \tag{1}$$

where $Q$ represents the incoming solar radiation ($W/m^2$), corresponding to a quarter of the solar constant. The function $s(x^0)$ represents the solar energy distribution as a function of latitude, normalized to unity. The term $\alpha(x^0)$ denotes the albedo, which is the fraction of solar radiation reflected back into space. The relation $x^0 = \sin(\text{latitude})$ expresses the link between latitude and position on the Earth's sphere. The term $A + By$ represents the linearized form of the Earth's infrared radiation emission into space (modeling the outgoing longwave radiation emitted by the Earth-atmosphere system), which indicates that the higher the Earth's surface temperature, the greater the outgoing radiation. This formulation is adjusted based on observational data of outgoing longwave radiation. The parameters are given as follows: $A = 202\ W/m^2$ represents the infrared emission parameter, and $B = 1.90\ W/m^2.\check{r}C^{-1}$ is the thermal loss coefficient [32, 33].

This model represents a control problem formulation for climate dynamics described by a parabolic-type equation, where temperature is influenced by variations in albedo and solar distribution as a function of latitude. The earliest studies that modeled temperature variations at the Earth's surface [10, 51], introducing one-dimensional energy balance models based on radiative equilibrium and the effect of albedo. Subsequently, temperature variations were described as a function of space-time variables and modeled using a parabolic equation, as highlighted in [41]. The emission of infrared radiation by the Earth, with coefficients $A$ and $B$ based on satellite observations, was studied by [45, 55]. The integration of optimal control theory into these models allows for the study of mechanisms to mitigate global warming. Some studies explore this approach through local or global modifications of Earth's albedo [29, 37].

These studies intersect applied mathematics (PDEs, control theory) and climate physics. It is important to note that surface temperature on Earth varies with latitude, being higher near the equator and lower at the poles. This variation is due to the angle of incidence of solar radiation as well as changes in albedo with latitude (higher albedo at the poles and lower at the equator). Snow-covered or icy surfaces have a high albedo, whereas oceanic or forested areas have a lower albedo. Albedo is a value between 0 and 1, representing the fraction of reflected energy relative to incident solar energy. The Earth's average albedo is approximately 30% of incident solar energy, meaning that the remaining 70% is absorbed by the Earth [24].

To control Earth's albedo and mitigate the effects of global warming, several approaches are being considered. Technological methods, such as injecting aerosols into the stratosphere or deploying artificial reflectors in space, aim to increase the reflection of solar radiation [34]. On a smaller scale, modifications to land surfaces—such as the use of white roofs or reflective management of agricultural soils—have been explored [3]. Additionally, natural solutions offer a more sustainable alternative: reforestation, restoration of grasslands and wetlands, and conservation of glaciers can enhance albedo while preserving biodiversity and ecosystems [13, 25]. These approaches help protect the environment, though their direct impact on global albedo remains limited compared to technological interventions.

The time required to observe changes through albedo control depends on several factors, including the magnitude of the albedo change, local climatic conditions, and the sensitivity of the climate system to these modifications. Generally, significant changes in albedo can lead to noticeable temperature variations over timescales ranging from a few months to several years [24]. Climate models and numerical simulations, such as those we use, are valuable tools for estimating these timescales and understanding the underlying dynamics.

Below are graphical illustrations representing solar distribution and albedo variation with latitude:

The study of the null controllability of the model problem at the final time $T$, for all $y_0 \in L^2(\Omega)$ and $u \in L^2(]0,T[\times\omega)$ such that the solution $y_u$ of eq. (1) satisfies $y_u(T,x) = 0$, has led us to define the following optimal control problem:

$$\min_{u\in\mathscr{U}} J(u) = \frac{1}{2}\iint_{]0,T[\times\omega} |u(t,x)|^2\,dt\,dx + \frac{1}{2}\|y_u(T,x)\|^2_{L^2(\Omega)}. \tag{2}$$

where $\mathscr{U}$ is the set of admissible controls given by:

$$\mathscr{U} = \{u \in L^2(]0,T[\times\omega);\ y_u(T,y_0) = 0\}. \tag{3}$$

We study the null controllability of system eq. (1) through the following theorem:

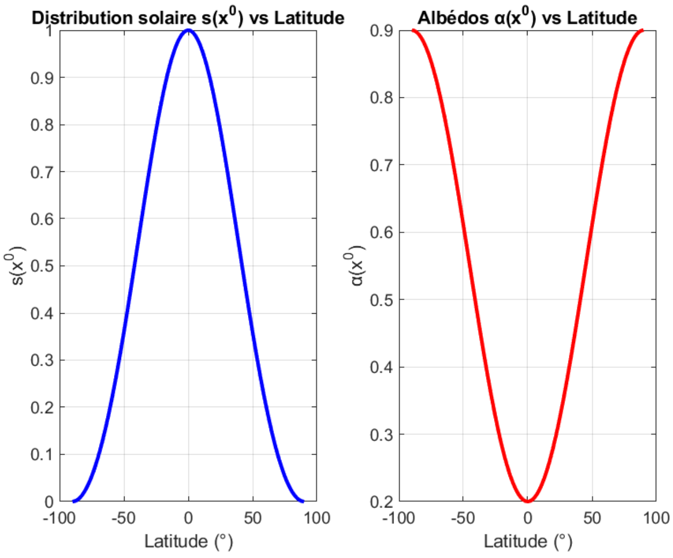


**Fig. 1.** Solar Distribution and Albedo

**Theorem 2.1.**
*For any $y_u \in C^0(0,T,L^2(\Omega)) \cap L^2(0,T,H_0^1(\Omega))$, a solution of eq. (1) associated with $y_0$, $u$ satisfies $y_u(T,x) = 0$.*
*Then, there exists a constant $C_{obs} > 0$ such that the inequality*

$$\| \varphi(0) \|^2_{L^2(\Omega)} \leqslant C_{obs} \iint_{]0,T[\times\omega} |\varphi(t,x)|^2 dt dx$$

*holds for every solution $\varphi \in C^0(0,T,L^2(\Omega)) \cap L^2(0,T,H_0^1(\Omega))$ of the adjoint problem associated with $\varphi_0 \in L^2(\Omega)$.*

To prove theorem 2.1 , we begin by defining the adjoint problem of eq. (1), which is given by the following system:

$$\begin{cases} -\frac{\partial \varphi}{\partial t} - \Delta\varphi + B\varphi = 0 & \forall (t,x) \in ]0,T[\times\Omega \\ \varphi(T,x) = y_u(T,x) & \forall x \in \Omega \\ \varphi(t,x) = 0 & \forall (t,x) \in ]0,T[\times\partial\Omega. \end{cases} \tag{4}$$

and

$$u(t,x) = QS(x)\alpha(x)\mathbf{1}_\omega \varphi(t,x).$$

Thus, the observability inequality is a consequence of the global Carleman inequality for the adjoint system, leading to the introduction of the auxiliary function $\zeta \in C^2(\bar{\Omega})$ satisfying the following conditions:

$$\begin{cases} \zeta(x) > 0 & \forall x \in \Omega \\ \zeta(x) = 0 & \forall x \in \partial\Omega \\ \nabla\zeta \neq 0 & \forall x \in \overline{\Omega\backslash\omega}. \end{cases} \tag{5}$$

For the proof of existence, see ([2]).
Let $k^0 > 0$ such that $k^0 \geq 5\max_{\bar{\Omega}} \zeta - 6\min_{\bar{\Omega}} \zeta$, $\theta^0 = \zeta + k^0$ and $\theta^1 = \frac{5}{4}\max_{\bar{\Omega}} \theta^0$.
We also introduce

$$\vartheta(t,x) = \frac{\vartheta^0}{t(T-t)} \tag{6}$$

where $\vartheta^0 = e^{\lambda\theta^1} - e^{\lambda\theta^0}$ and $\lambda >> 0$.

We also consider the following proposition, which provides the adapted Carleman inequality:

**Proposition 2.1** ([15, 18]).
*There exist constants $C^*>0$ and $\sigma>0$ (depending only on $\Omega$ and $\omega$) such that*

$$s\iint_\Lambda e^{-2s\vartheta}t^{-1}(T-t)^{-1}|\nabla\varphi|^2dtdx+s^3\iint_\Lambda e^{-2s\vartheta}t^{-3}(T-t)^{-3}|\varphi|^2dtdx$$
$$\leq C^*\left[\iint_\Lambda e^{-2s\vartheta}|B\varphi|^2dtdx+s^3\iint_{]0,T[\times\omega}e^{-2s\vartheta}t^{-3}(T-t)^{-3}|\varphi|^2dtdx\right] \tag{7}$$

*for all $s_1=\sigma_1(\Omega,\omega)(T+T^2)$ ($\varphi$ is a solution of eq. (4) with $\varphi(T,.)\in L^2(\Omega)$).*

*Proof.* We estimate

$$\iint_\Lambda e^{-2s\vartheta}|B\varphi|^2dtdx\leq 2^{-6}T^6B^2\iint_\Lambda e^{-2s\vartheta}t^{-3}(T-t)^{-3}|\varphi|^2dtdx \tag{8}$$

where

$$2^{-6}T^6B^2C^*\leq\frac{1}{4}s^3 \tag{9}$$

Thus, from proposition 2.1, we deduce

$$\iint_\Lambda e^{-2s\vartheta}t^{-1}(T-t)^{-1}|\nabla\varphi|^2dtdx\leq C^*s^2\iint_{]0,T[\times\omega}e^{-2s\vartheta}t^{-3}(T-t)^{-3}|\varphi|^2dtdx \tag{10}$$

with

$$s\geq s_2=\max\{s_1,2^{-\frac{4}{3}}C^{*\frac{1}{3}}T^2B^{\frac{2}{3}}\} \tag{11}$$

□

Estimation of the weight $s$ eq. (10)

**Lemma 2.1.**
*The following inequalities hold:*

$$e^{-2s\vartheta}t^{-3}(T-t)^{-3}\leq 2^6T^{-6}e^{-C'sT^{-2}}\qquad\forall(t,x)\in[0,T]\times\Omega \tag{12}$$

$$e^{-2s\vartheta}t^{-1}(T-t)^{-1}\geq\frac{16}{3}e^{-C''sT^{-2}}\qquad\forall(t,x)\in[\frac{T}{4},\frac{3T}{4}]\times\bar{\Omega} \tag{13}$$

*for all*

$$s\geq s_3=\{s_2,3T^2(8\min_{x\in\bar{\Omega}}\alpha_0(x))^{-1}\} \tag{14}$$

*with $C',\ C''>0$.*

*Proof.* For $t\in[0,T]$, we have $t(T-t)\leq\frac{T^2}{4}$. Thus:

$$\vartheta(t,x)\geq\frac{4}{T^2}\left(e^{\lambda\frac{5}{4}\max_{\bar{\Omega}}(\zeta+k^0)}-e^{\lambda(\zeta(x)+k^0)}\right).$$

Setting $C'=8\min_{x\in\bar{\Omega}}\left(e^{\lambda\frac{5}{4}\max_{\bar{\Omega}}(\zeta+k^0)}-e^{\lambda(\zeta+k^0)}\right)$, we obtain:

$$e^{-2s\vartheta(t,x)}\leq\exp\left(-C'sT^{-2}\right).$$

Since $t(T-t)\leq\frac{T^2}{4}$, we have $t^{-3}(T-t)^{-3}\leq 2^6T^{-6}$. Thus:

$$e^{-2s\vartheta}t^{-3}(T-t)^{-3}\leq 2^6T^{-6}\exp(-C'sT^{-2}),$$

which proves eq. (12).

For $t\in\left[\frac{T}{4},\frac{3T}{4}\right]$, we have $t(T-t)\geq\frac{T^2}{16}$. Consequently:

$$\vartheta(t,x)\leq\frac{16}{T^2}\left(e^{\lambda\frac{5}{4}\max_{\bar{\Omega}}(\zeta+k^0)}-e^{\lambda(\zeta+k^0)}\right).$$

Setting $C'' = 32\max_{x\in\bar{\Omega}}\left(e^{\lambda\frac{5}{4}\max_{\bar{\Omega}}(\zeta+k^0)} - e^{\lambda(\zeta+k^0)}\right)$, we have:

$$e^{-2s\vartheta(t,x)} \geq \exp\left(-C''sT^{-2}\right).$$

For the factor $t^{-1}(T-t)^{-1}$, since $t\in\left[\frac{T}{4},\frac{3T}{4}\right]$, we have $t^{-1}(T-t)^{-1} \geq \left(\frac{T}{4}\right)^{-2} = 16T^{-2}$. Thus:

$$e^{-2s\vartheta}t^{-1}(T-t)^{-1} \geq 16T^{-2}\exp(-C''sT^{-2}).$$

Choosing a constant $\frac{16}{3}$, we get:

$$e^{-2S\vartheta}t^{-1}(T-t)^{-1} \geq \frac{16}{3}e^{-C''sT^{-2}},$$

which proves eq. (13). □

**Remark 2.1.**
Given relations eqs. (9), (11) and (14), we take

$$s = s_3 = C(T + (1+B^2)T^2). \tag{15}$$

**Proof of theorem 2.1**

We multiply system eq. (4) by $\varphi$ and integrate over $\Omega$ using Green's formula. This gives us:

$$-\frac{1}{2}\frac{d}{dt}\int_\Omega |\varphi(t,x)|^2dx + \int_\Omega |\nabla\varphi(t,x)|^2dx + B\int_\Omega |\varphi(t,x)|^2dx = 0. \tag{16}$$

Next, applying Poincaré's inequality, we obtain:

$$-\frac{1}{2}\frac{d}{dt}\int_\Omega |\varphi(t,x)|^2dx + K\int_\Omega |\varphi(t,x)|^2 + B\int_\Omega |\varphi(t,x)|^2dx \leq 0. \tag{17}$$

Rearranging this inequality:

$$\frac{-1}{2}\frac{d}{dt}\left(e^{-2(B+K)t}\int_\Omega |\varphi(t,x)|^2dx\right) \leq 0. \tag{18}$$

At this stage, we integrate inequality eq. (18) over the interval $[\frac{T}{4},t]$, where $t\in[\frac{T}{4},\frac{3T}{4}]$, which gives us:

$$e^{-2(B+K)(\frac{T}{4}-t)}\int_\Omega |\varphi(\frac{T}{4},x)|^2dx \leq \int_\Omega |\varphi(t,x)|^2dx, \tag{19}$$

$$e^{(B+K)(T)}\int_\Omega |\varphi(\frac{T}{4},x)|^2dx \leq \int_\Omega |\varphi(t,x)|^2dx. \tag{20}$$

By integrating this inequality over the interval $[\frac{T}{4},\frac{3T}{4}]$, we obtain:

$$Te^{(B+K)(T)}\int_\Omega |\varphi(\frac{T}{4},x)|^2dx \leq \int_{\frac{T}{4}}^{\frac{3T}{4}}\int_\Omega |\varphi(t,x)|^2dtdx. \tag{21}$$

Now, we combine eqs. (10), (12) and (13) and apply Poincaré's inequality to obtain the following inequality:

$$\int_{\frac{T}{4}}^{\frac{3T}{4}}\int_\Omega |\varphi(t,x)|^2dtdx \leq \frac{1}{K}\exp\left(C\left(1+\frac{1}{T}+(B+K)^{\frac{2}{3}}\right)\right)\iint_{]0,T[\times\omega}|\varphi(t,x)|^2dtdx. \tag{22}$$

This allows us to conclude with the relation:

$$Te^{(B+K)(T)}\int_\Omega |\varphi(\frac{T}{4},x)|^2dx \leq \frac{1}{K}\exp\left(C\left(1+\frac{1}{T}+(B+K)^{\frac{2}{3}}\right)\right)\iint_{]0,T[\times\omega}|\varphi(t,x)|^2dtdx. \tag{23}$$

We also integrate relation eq. (18) over the interval $[0,\frac{T}{4}]$, which gives

$$e^{(B+K)(\frac{T}{2})}\int_\Omega |\varphi(0,x)|^2dx \leq \int_\Omega |\varphi(\frac{T}{4},x)|^2dx. \tag{24}$$

Finally, by combining eqs. (23) and (24), we obtain the observability inequality:

$$\|\varphi(0)\|_{L^2(\Omega)} \leq \frac{1}{KT}\exp\left(C\left(1+\frac{1}{T}+(B+K)^{\frac{2}{3}}-\frac{3}{2}(B+K)T\right)\right)\iint_{]0,T[\times\omega}|\varphi(t,x)|^2dtdx. \tag{25}$$

## 3. Numerical Resolution

Consider the following problem:

$$\min_{u\in\mathscr{U}} J(u) = \frac{1}{2}\iint_{]0,T[\times\omega} |u(t,x)|^2\,dt\,dx + \frac{1}{2}\int_{-1}^{1} |y_u(T,x)|^2\,dx. \tag{26}$$

$$\begin{cases} \frac{\partial y}{\partial t} - \frac{\partial^2 y}{\partial x^2} + A + By = QS(x^0)[1-\alpha(x^0)\mathbf{1}_\omega u] & \forall (t,x)\in[0,T]\times[-1,1] \leqslant x < \\ y(0,x) = y_0(x) & \forall x\in[-1,1] \leqslant x < \\ y(t,-1) = y(t,1) = 0 & \forall t\in[0,T] \leqslant x < \end{cases} \tag{27}$$

We propose a numerical resolution of the problem by combining **the spectral method** and **the Adomian decomposition method**, relying on the variational formulation [9, 53].

Let $z$ be a test function. The variational formulation associated with the problem described by the state equation, with the initial and boundary conditions, is written as

$$\begin{aligned} \int_{-1}^{1} y(T;x)z(T;x)\,dx &= \int_{-1}^{1} y(0)z(0;x)\,dx + \int_0^T\int_{-1}^{1} y\frac{\partial z}{\partial x}\,dt\,dx \\ &- \int_0^T\int_{-1}^{1}\frac{\partial y}{\partial x}\frac{\partial z}{\partial x}\,dt\,dx \qquad (28)\\ &- B\int_0^T\int_{-1}^{1} y(t,x)z(t,x)\,dt\,dx \\ &+ \int_0^T\int_{-1}^{1} QS(x^0)[1-\alpha(x^0)\mathbf{1}_\omega u]z(t;x)\,dt\,dx. \qquad (29) \end{aligned}$$

We seek an approximate solution in the interval $[0;T]$, which we decompose into subintervals

$$[0;T] = \bigcup_{k\in\mathbb{N}} [t_k, t_{k+1}].$$

We approximate the solution $y$ in the form

$$y^N = \sum_{j=0}^{N} y_j(t)\psi_j(x). \tag{30}$$

Similarly, we approximate the control $u$ by

$$u^N = \sum_{j=0}^{N} u_j(t)\psi_j(x). \tag{31}$$

By choosing the test function in the form $z(t,x) = \psi_i(x)$ for $i = 0,\dots,N$, and substituting into section 3, we obtain for all $\tau\in[0;T]$

$$\begin{aligned} \sum_{j=0}^{N} y_j(\tau)\int_{-1}^{1}\psi_j(x)\psi_i(x)\,dx &= \sum_{j=0}^{N} y_j(0)\int_{-1}^{1}\psi_j(x)\psi_i(x)\,dx - B\sum_{j=0}^{N}\int_0^\tau y_j(t)\int_{-1}^{1}\psi_j(x)\psi_i(x)\,dx \\ &- \sum_{j=0}^{N}\int_0^\tau y_j(t)\int_{-1}^{1}\psi_j'(x)\psi_i'(x)\,dx \\ &+ \int_0^\tau\int_{-1}^{1} QS(x^0)[1-\alpha(x^0)\mathbf{1}_\omega\sum_{j=0}^{N} u_j(t)\psi_j(x)]\psi_i(x)\,dt\,dx. \end{aligned} \tag{32}$$

We use the orthogonality relations of the basis functions

$$\int_{-1}^{1}\psi_j(x)\psi_i(x)\,dx = \delta_{ij} = \begin{cases} 1, & \text{if } i = j, \\ 0, & \text{otherwise.}\end{cases}$$

Furthermore, we define the differential matrix

$$d_{ij} = \int_{-1}^{1} \psi'_j(x)\psi'_i(x)\,dx.$$

Thus, we obtain the following expression

$$\begin{aligned} y_i(\tau) &= y_i(0) - B\int_0^{\tau} y_i(t)\,dt - \sum_{j=0}^{N} d_{ij}\int_0^{\tau} y_j(t)\,dt \\ &- \sum_{j=0}^{N}\int_0^{\tau} u_j(t)\,dt\int_{-1}^{1} QS(x^0)\alpha(x^0)\mathbf{1}_{\omega}\psi_j(x)\psi_i(x)\,dx \\ &+ \int_0^{\tau}\int_{-1}^{1}(QS(x^0)-A)\psi_i(x)\,dt\,dx. \end{aligned} \tag{33}$$

This equation is known as the **canonical form of Adomian**.
Finally, we decompose the solution $y_i(t)$ and the control $u_j(t)$ in the form of infinite series

$$y_i(t) = \sum_{n=0}^{\infty} y_{i;\,n}(t), \quad u_j(t) = \sum_{n=0}^{\infty} u_{j;\,n}(t).$$

From the previously obtained relation, we have

$$\begin{aligned} \sum_{n=0}^{\infty} y_{i;\,n}(\tau) &= y_i(0) - B\int_0^{\tau}\sum_{n=0}^{\infty} y_{i;\,n}(t)\,dt - \sum_{j=0}^{N} d_{ij}\int_0^{\tau}\sum_{n=0}^{\infty} y_{j;\,n}(t)\,dt \\ &- \sum_{j=0}^{N}\int_0^{\tau}\sum_{n=0}^{\infty} u_{j;\,n}(t)\,dt\int_{-1}^{1} QS(x^0)\alpha(x^0)\mathbf{1}_{\omega}\psi_j(x)\psi_i(x)\,dx \\ &+ \int_0^{\tau}\int_{-1}^{1}(QS(x^0)-A)\psi_i(x)\,dt\,dx. \end{aligned} \tag{34}$$

Thus, the following resolution algorithm is obtained

$$\begin{cases} y_{i;0}(t) = y_i(0) + \tau\displaystyle\int_{-1}^{1}(QS(x^0)-A)\psi_i(x)\,dx, \\ y_{i;n+1}(t) = -B\displaystyle\int_0^{\tau} y_{i;n}(t)\,dt - \sum_{j=0}^{N} d_{ij}\int_0^{\tau} y_{j;n}(t)\,dt \\ \quad -\sum_{j=0}^{N}\int_0^{\tau} u_{j;0}(t)\,dt\int_{-1}^{1} QS(x^0)\alpha(x^0)\mathbf{1}_{\omega}\psi_j(x)\psi_i(x)\,dx. \end{cases} \tag{35}$$

By applying this algorithm, we obtain

$$\begin{aligned} y_{i;1}(t) &= \Big[-By_i(0) - \sum_{j=0}^{N} d_{ij}y_j(0) - \sum_{j=0}^{N} u_j(0)\int_{-1}^{1} QS(x^0)\alpha(x^0)\mathbf{1}_{\omega}\psi_j(x)\psi_i(x)\,dx\Big]t \\ &+ \Big[\Big(B - \sum_{j=0}^{N} d_{ij}\Big)\int_{-1}^{1}(QS(x^0)-A)\psi_i(x)\,dx\Big]t^2. \end{aligned} \tag{36}$$

Thus, at each iteration

$$\begin{aligned} y_{i;1}(t_{k+1}) &= \Big[-By_i(t_k) - \sum_{j=0}^{N} d_{ij}y_j(t_k) - \sum_{j=0}^{N} u_j(t_k)\beta_{ij}\Big](t_{k+1}-t_k) \\ &+ \Big(B - \sum_{j=0}^{N} d_{ij}\Big)\eta_i(t_{k+1}-t_k)^2. \end{aligned} \tag{37}$$

where

$$\beta_{ij} = \int_{-1}^{1} QS(x^0)\alpha(x^0)\mathbf{1}_{\omega}\psi_j(x)\psi_i(x)\,dx, \quad \eta_i = \int_{-1}^{1}(QS(x^0)-A)\psi_i(x)\,dx.$$

Approximation of the solution

$$\begin{aligned} y_i(t_{k+1}) &= y_i(t_k) + \Big[\eta_i - By_i(t_k) - \sum_{j=0}^{N} d_{ij} y_j(t_k) - \sum_{j=0}^{N} u_j(t_k)\beta_{ij}\Big](t_{k+1}-t_k) \\ &+ \Big(B - \sum_{j=0}^{N} d_{ij}\Big)\eta_i (t_{k+1}-t_k)^2 + o(\Delta t). \end{aligned} \tag{38}$$

Approximation of the functional

$$\begin{aligned} J^N &\approx \frac{1}{2}\int_{-1}^{1} |y_{u^N}^N(t_{k+1},x)|^2\,dx + \frac{1}{2}\int_{t_k}^{t_{k+1}}\int_{-1}^{1} |u^N(t,x)|^2\,dt\,dx \\ &\approx \frac{1}{2}\sum_{i,j=0}^{N} y_i(\tau)y_j(\tau)\int_{-1}^{1}\psi_i(x)\psi_j(x)\,dx + \frac{1}{2}\sum_{i,j=0}^{N}\int_0^{\tau} u_i(t)u_j(t)\,dt\int_{-1}^{1}\psi_i(x)\psi_j(x)\,dx \\ &\approx \frac{1}{2}\sum_{i=0}^{N} y_i^2(\tau) + \frac{1}{2}\sum_{i=0}^{N}\int_0^{\tau} u_i^2(t)\,dt. \end{aligned} \tag{39}$$

We define the vectors

$$Y = \Big[y_0(t),\dots,y_N(t)\Big]^t, \quad U = \Big[u_0(t),\dots,u_N(t)\Big]^t. \tag{40}$$

Thus, relation section 3 can be written in discrete form as

$$J^{MN} \approx \frac{\delta t}{2}\sum_{k=0}^{M}\Big[\Big(Y^k(t_{k+1})\Big)^t Y^k(t_{k+1}) + \Big(U^k(t_{k+1})\Big)^t U^k(t_{k+1}) + \Big(U^k(t_k)\Big)^t U^k(t_k)\Big]. \tag{41}$$

### 3.1. Numerical Simulation

In this section, we present the numerical simulation of the uncontrolled temperature at the Earth's surface, followed by that of the optimal control and the controlled temperature at the Earth's surface for specific regions in $2D$ and $3D$. The values of $M$, $N$, and $T$ correspond to the truncation parameters for the time variable, the spatial variable (latitude), and the final time, respectively. This simulation is carried out in the MATLAB environment.

#### 3.1.1. Evolution of the Uncontrolled Temperature

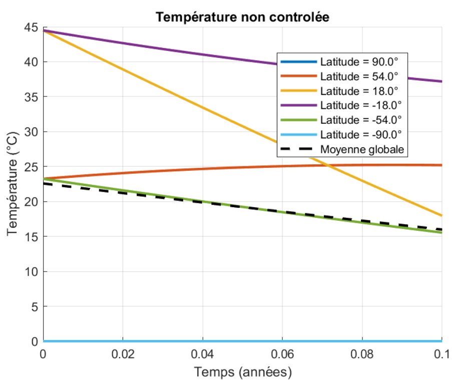


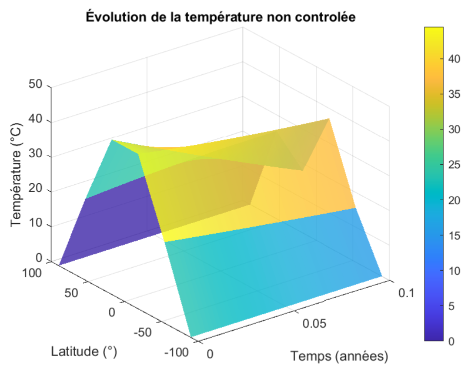


**Fig. 2.** Uncontrolled temperature for $N = 5$, $M = 1000$, $T = 0.1$.

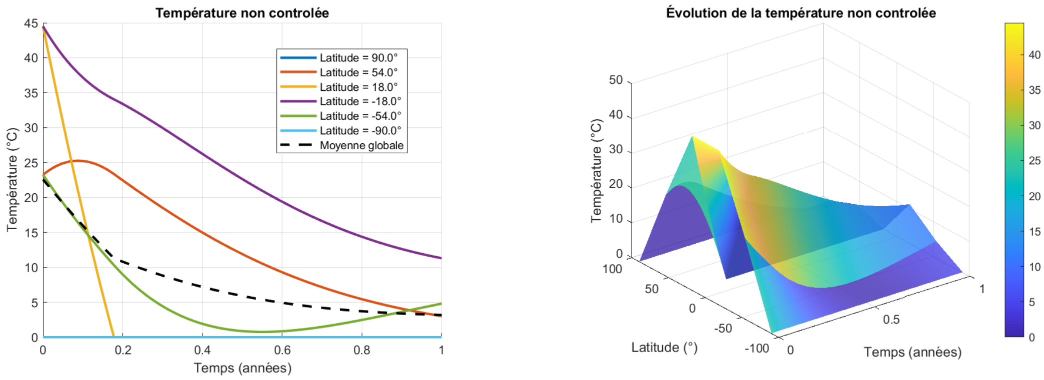


**Fig. 3.** Uncontrolled temperature for $N = 5,\ M = 1000,\ T = 1$.

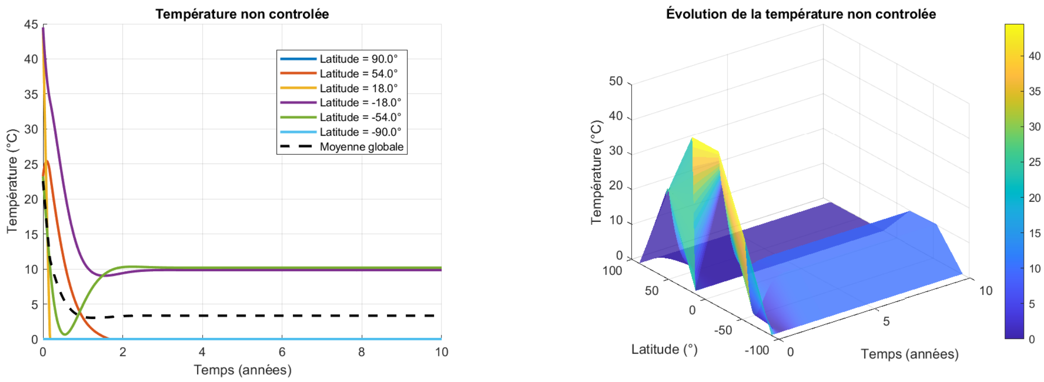


**Fig. 4.** Uncontrolled temperature for $N = 5,\ M = 1000,\ T = 10$.

#### 3.1.2. Evolution of the Controlled Temperature

**For the control domain of latitude from $-20°$ to $20°$**

**Table 1.** Summary of results

| **Final_Time** | 0.1 | 1 | 10 |
|---|---|---|---|
| **Min_Temperature** | 0 | 0 | 0 |
| **Max_Temperature** | 31.678 | 6.0341 | 2.9521 |
| **Global_Mean_Temperature** | 10.539 | 1.0253 | 0.98109 |
| **Control_Mean_Temperature** | 21.234 | 3.017 | 1.4673 |
| **Final_Mean_Control** | 0.17271 | 0.17271 | 0.17271 |
| **Mean_Albedo** | 0.26684 | 0.26684 | 0.26684 |
| **Cost_Function** | 112.64 | 274.4 | 358.51 |

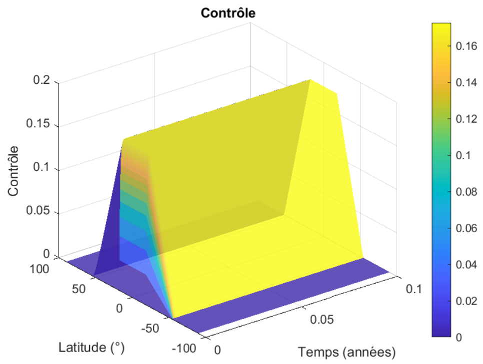


**Fig. 5.** Controlled temperature for $N = 5,\ M = 1000,\ T = 0.1$.

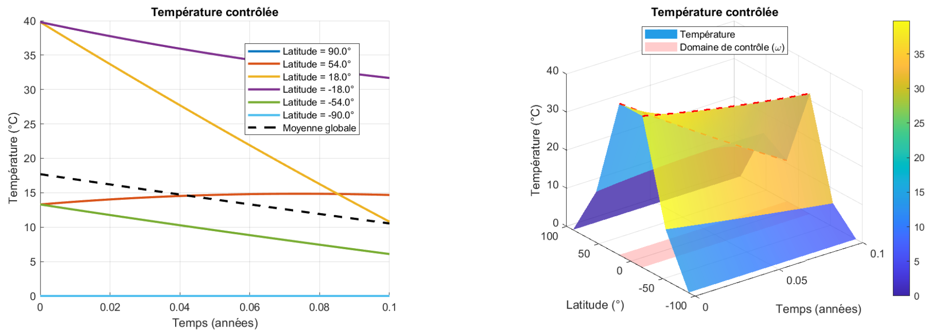


**Fig. 6.** Controlled temperature for $N = 5,\ M = 1000,\ T = 0.1$.

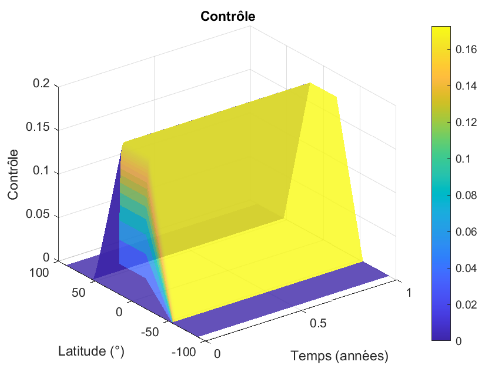


**Fig. 7.** Controlled temperature for $N = 5,\ M = 1000,\ T = 1$.

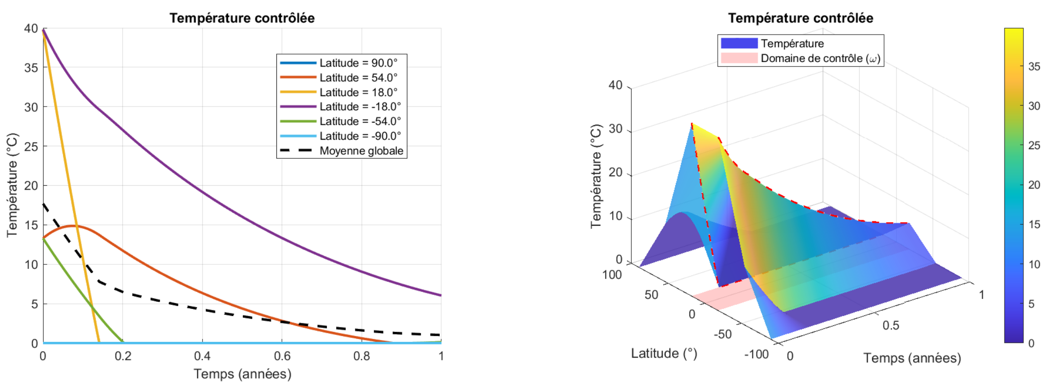


**Fig. 8.** Controlled temperature for $N = 5,\ M = 1000,\ T = 1$.

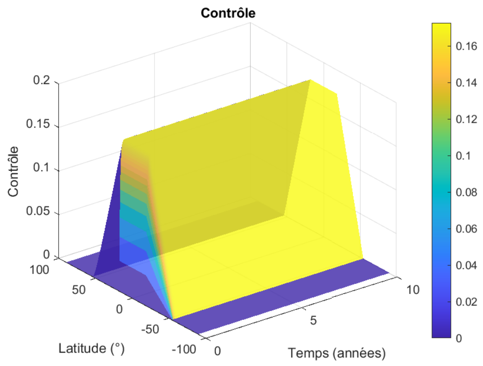


**Fig. 9.** Controlled temperature for $N = 5,\ M = 1000,\ T = 10$.

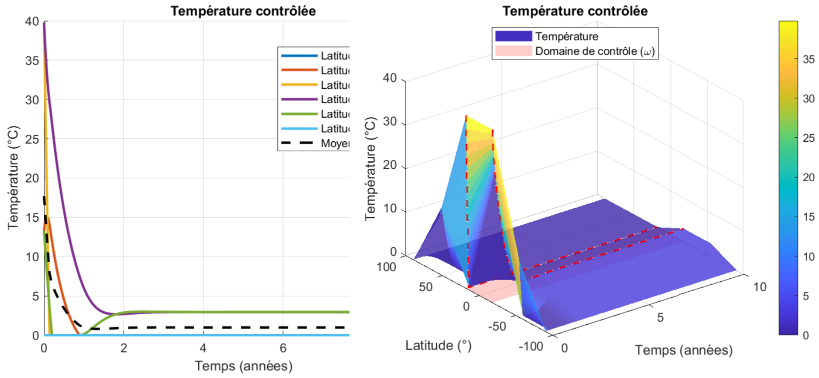


**Fig. 10.** Controlled temperature for $N = 5,\ M = 1000,\ T = 10$.

### For the control domain of latitude from 20° to 60°

**Table 2.** Summary of results

| | | | |
|---|---|---|---|
| **Final_Time** | 0.1 | 1 | 10 |
| **Min_Temperature** | 0 | 0 | 0 |
| **Max_Temperature** | 31.664 | 5.9714 | 2.9879 |
| **Global_Mean_Temperature** | 10.534 | 1.0168 | 0.97946 |
| **Control_Mean_Temperature** | 14.676 | 0 | 0 |
| **Final_Mean_Control** | 0.043981 | 0.043981 | 0.043981 |
| **Mean_Albedo** | 0.65816 | 0.65816 | 0.65816 |
| **Cost_Function** | 112.59 | 273.77 | 357.03 |

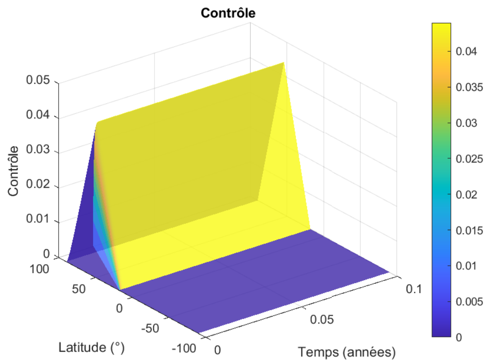


**Fig. 11.** Controlled temperature for $N = 5,\ M = 1000,\ T = 0.1$.

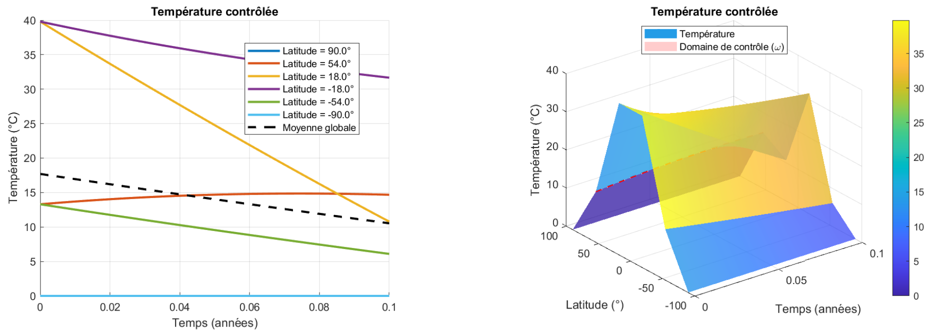


**Fig. 12.** Controlled temperature for $N = 5,\ M = 1000,\ T = 0.1$.

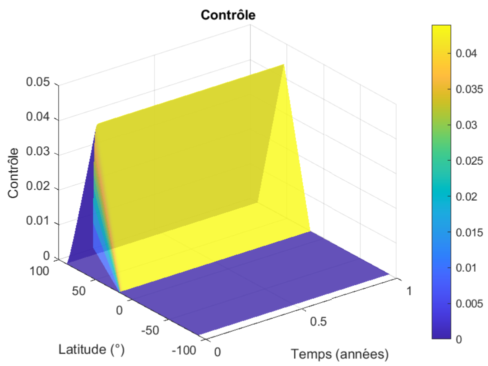


**Fig. 13.** Controlled temperature for $N = 5,\ M = 1000,\ T = 1$.

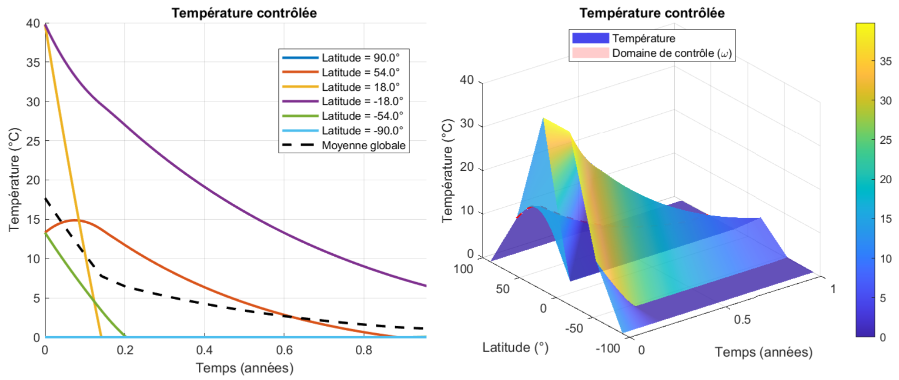


**Fig. 14.** Controlled temperature for $N = 5,\ M = 1000,\ T = 1$.

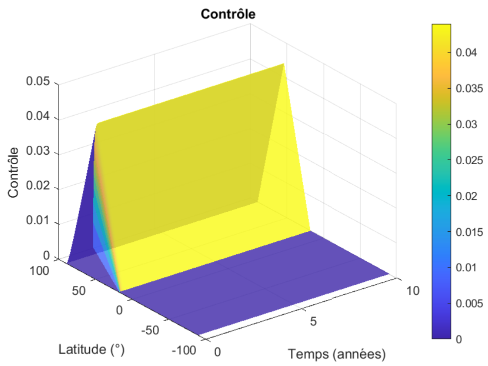


**Fig. 15.** Controlled temperature for $N = 5,\ M = 1000,\ T = 10$.

## For the control domain of latitude from $-60°$ to $-20°$

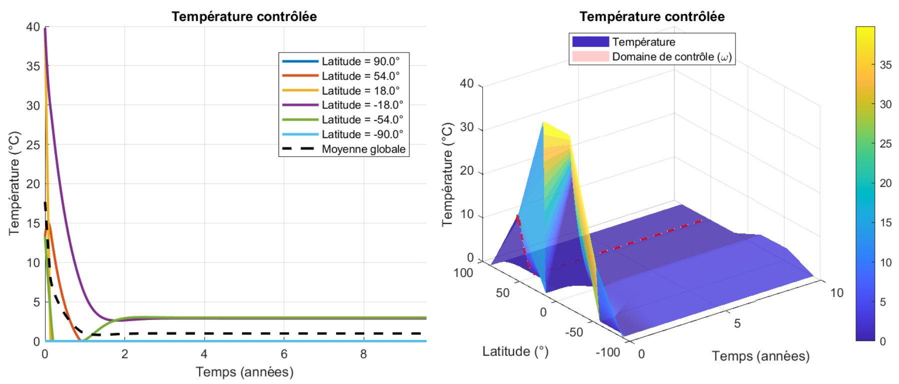


**Fig. 16.** Controlled temperature for $N = 5,\ M = 1000,\ T = 10$.

**Table 3.** Summary of results

| | | | |
|---|---|---|---|
| **Final_Time** | 0.1 | 1 | 10 |
| **Min_Temperature** | 0 | 0 | 0 |
| **Max_Temperature** | 31.664 | 5.9714 | 2.9879 |
| **Global_Mean_Temperature** | 10.534 | 1.0168 | 0.97946 |
| **Control_Mean_Temperature** | 6.0932 | 0.12962 | 2.9879 |
| **Final_Mean_Control** | 0.043981 | 0.043981 | 0.043981 |
| **Mean_Albedo** | 0.65816 | 0.65816 | 0.65816 |
| **Cost_Function** | 112.59 | 273.77 | 357.03 |

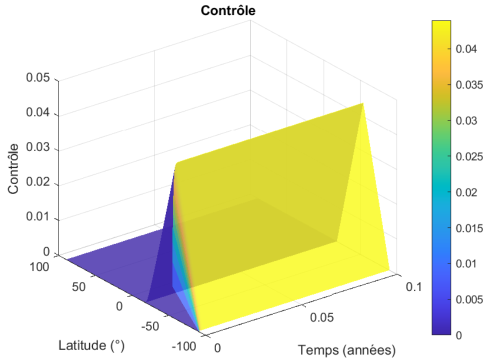


**Fig. 17.** Controlled temperature for $N = 5,\ M = 1000,\ T = 0.1$.

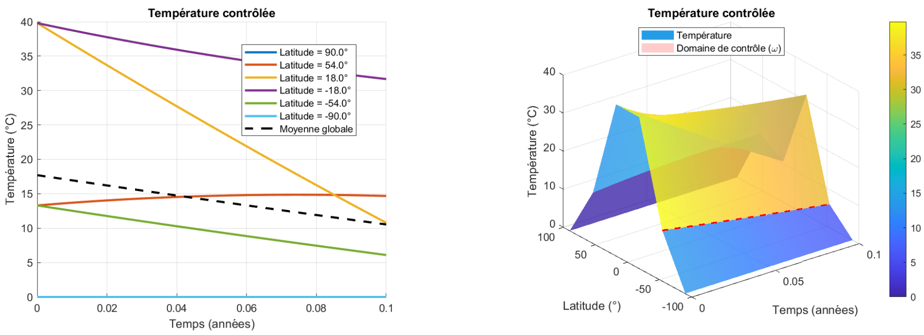


**Fig. 18.** Controlled temperature for $N = 5,\ M = 1000,\ T = 0.1$.

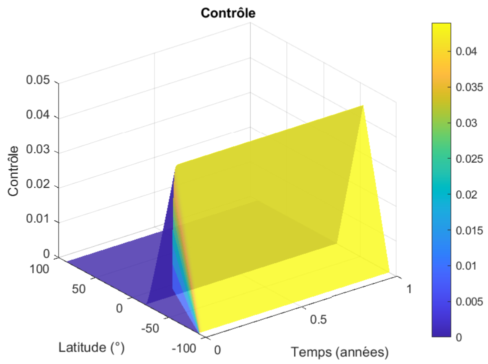


**Fig. 19.** Controlled temperature for $N = 5,\ M = 1000,\ T = 1$.

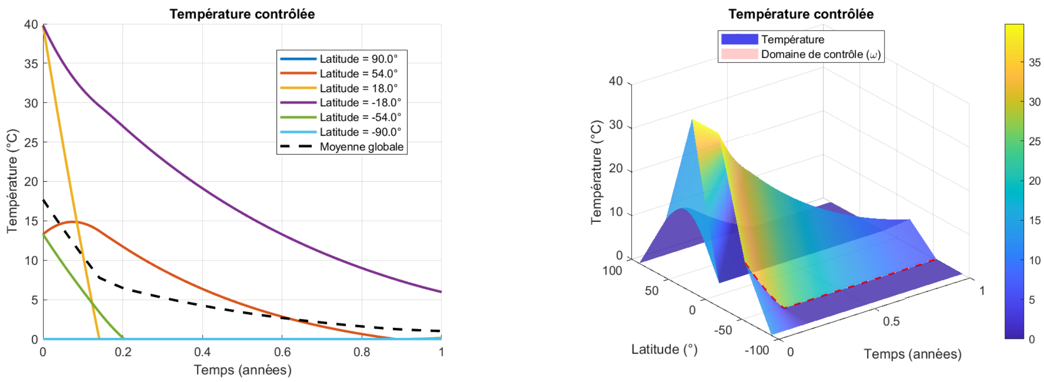


**Fig. 20.** Controlled temperature for $N = 5,\ M = 1000,\ T = 1$.

## 4. Discussion

The general observation from this numerical simulation allows us to conclude that the temperature distribution at the Earth's surface follows a decreasing function as we move away from the equator, for different latitudes. Areas with higher albedo (such as polar regions) have lower temperatures compared to regions with lower albedo. The impact on albedo has a significant effect on temperature variations in the controlled region, as we observe a decrease in temperature compared to the uncontrolled case. The graphs (figs. 3, 4, 6, 8, 12, 14, 16, 18 and 20 and **??**) show that after a certain amount of time, the temperature reaches thermal equilibrium.

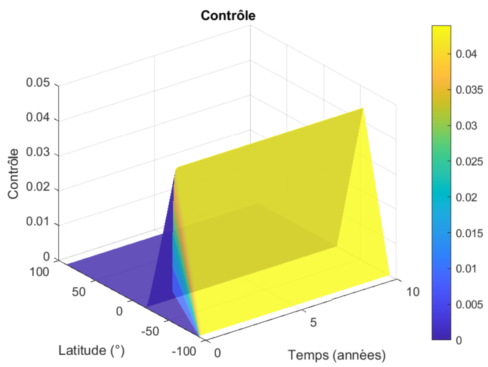


**Fig. 21.** Controlled temperature for $N = 5,\ M = 1000,\ T = 10$.

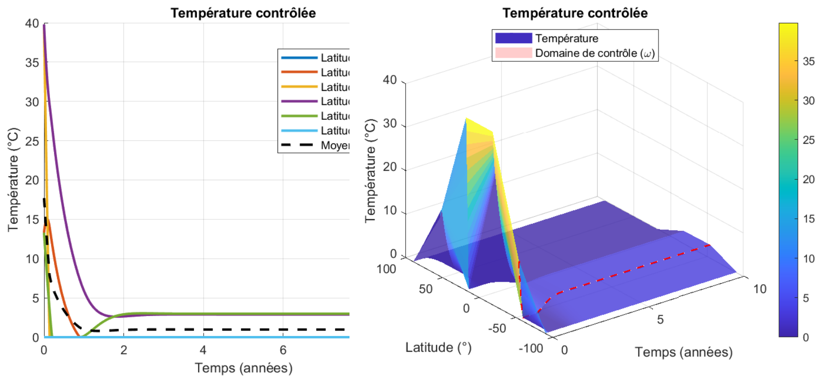


**Fig. 22.** Controlled temperature for $N = 5,\ M = 1000,\ T = 10$.

## 5. Conclusion

Our study focused on the mathematical study and numerical simulation of a controlled climate model. We began by presenting and reviewing literature on the model and then demonstrated its controllability to zero using Carleman's inequality.

The following part dealt with a numerical solution by coupling Adomian's decomposition method and the spectral method for the model problem, followed by a test problem that was numerically simulated. Finally, the coupling of Adomian's decomposition method and the spectral method proved to be highly effective in solving this problem.

## References

[1] A.S. Ackleh and B.G. Fitzpatrick, *Approximation and parameter estimation problems for Algal Aggregations models.*Maths.Models. Methods in Appl. Science 4(3) (1994).
[2] A. Fursikov and O. Yu. Imanuvilov, Controllability of Evolution Equations. 34, Seoul National University, Korea, 1996.
[3] Akbari, H., Menon, S., and Rosenfeld, A., Global cooling: Increasing world-wide urban albedos to offset CO2. Climatic Change, 2009.
[4] Ammari et al., Mathematical Modeling in Diffusion Problems (2022).
[5] Balira Ousmane KONEF, *Nouvelles méthodes mathématiques Alienor et Adpmian, pour la biomedécine.* Université de Ouagadougou, Thèse,2005.
[6] B. Fornberg, *A Practical Guide to Pseudospectral Methods.* Cambridge University Press, Cambridge, UK. 1996.
[7] B. Fornberg, *On A Fourier Method for the Integration of Hyperbolic Problems*, SIAM J (1975).
[8] Bisso Saley, *Résolution et simulation numérique d'un problème de contrôle optimale gouverné par des équations aux dérivées partielles de type diffusion-réaction issues de la modélisation mathématique en traitement du cancer du cerveau.* Université de Ouagadougou, Thèse, 2003.
[9] Bisso Saley and Benjamin Mampassi, *Solving large scale PDE optimisation problems with a decomposition scheme*, Pionner Scientific Publisher, 2011, 127-146.
[10] Budyko, M. I., The effect of solar radiation variations on the climate of the Earth. Tellus, 21(5), 1969, 611-619.
[11] Charles E. Graves, Wan-Hoo Lee, and Gerald R. North, New parametrizations and Sensitivites for simple climate models J. Geophys. Research, 98 (1993), 5025-5036.
[12] Crank, J., The Mathematics of Diffusion. Oxford University Press, (1975).
[13] Djamko Audrey, Estimation de l'effet biophysique albédo sur l'impact climatique de l'utilisation des cultures intermédiaires : Exemple de Cassur sur le site ICOS de Lonzée. Travail de fin d'études de Master en bioingénierie, sciences et technologies de l'environnement, 2021-2022.
[14] D. Gottlieb and J. S. Hesthaven, Spectral Methods for Hyperbolic Problems. Division of Applied Mathematics, Brown University, Box F, Providence, RI 02912, USA.
[15] E. Fernàndez-Cara, and E. Zuazua, The cost of approximate controllability for heat equations: The linear case, Advances in Differential Equations Volume 5 (4–6) April–June 2000, pp. 465–514.
[16] Erwin Kreyszig, Introductory Functional Analysis with Applications. Wiley, 1989.

[17] Evans. L. C., Partial Differential Equations (2019).
[18] Franck Boyer, *Controllability of linear parabolic equations and systems*, Université Paul Sabatier - Toulouse 3, Thèse, July 16, 2022.
[19] F. Lambert, Condition d'existence et d'unicité pour une équation différentielle fonctionnelle stochastique, Annales scientifiques de l'université de Clermont-Ferrand 2, tome 61, série Mathématiques, 1976, p. 43-70.
[20] F. M. White, Viscous Fluid Flow. McGraw-Hill. 1991.
[21] F. Tröltzsch, Optimal Control of Partial Differential Equations: Theory, Methods, and Applications. AMS, 2010.
[22] Haïm Brezis, Analyse fonctionnelle, théorie et applications, Masson, 1987.
[23] James Kigo , Mathew Kinyanjui, Roy Kiogora, Numerical Study on Turbulent Mixed Convection in a Greenhousewith Crop. Int. J. Adv. Appl. Math. and Mech. 10(1) (2022) 28– 38 (ISSN: 2347-2529).
[24] Gilles Delaygue et Benoît Urgelli, Étude des facteurs contrôlant la température de surface d'une planète. Centre Européen de Recherche et d'Enseignement des Géosciences de l'Environnement, Aix-en-Provence, ENS-Lyon/DGESCO, 15 février 2003.
[25] Griscom, B. W., et al., Natural climate solutions. Proceedings of the National Academy of Sciences, 2017.
[26] G. Szego, *Orthogonal Polynomials*. 4th Ed. American Mathematical Society, Colloquim Publication 23. Providence. 1975.
[27] H.T. Banks; On a variational approach to some parameter estimation problems on distributed parameter systems, springer lecture notes in control and info.Sci 75 (1985).
[28] Ionel Sorin CIUPERCA, Cours de contrôle optimal MAM5A, Polytech Lyon, 2022-2023.
[29] J. I. Diaz, On the Von Neumann problem and the approximate controlability of Stackelberg-Nash strategies for some environmental problems, Applied mathematics, Vol. 96(3), 2002, pp. 343-356.
[30] Jacques Lious Lions, Contrôle optimal de systèmes gouvernés par des équations aux dérivées partielles, Dunod, Paris, 1968.
[31] Jean-Michel Hervouet, Hydrodynamics of free surface flows. Elcetrcité de France (EDF), France.
[32] James Walsh, Climate Modeling in Differential Equations, The UMAP Journal 36 (4) (2015) 325-363.
[33] Ka Kit Tung, Simple climate modeling, AIMsciences.org, Vol. 7, 2007, pp. 651-660.;
[34] Keith, D. W., Parson, E., and Morgan, M. G., Research on global sun block needed now. Nature, 2017.
[35] KRUOCH Gael, DJIBO Moustapha, SALEY Bisso, Resolution and numerical simulation of a pollution model in a bounded domain of the atmosphere.Int.J.Adv.Appl.Math.and Mech.11(2)(2023)1-17 (ISSN:2347-2529).
[36] Lawrence C. Evans, Partial Differential Equations, Volume 19.American Mathematical Society, 2010.
[37] MacMartin, D. G., and Keith, D. W., Solar geoengineering and climate policy, Nature Reviews Earth and Environment, 1(1), 2019, 4-6.
[38] Maintine Bergounioux, Optimisation et contrôle des systèmes linéaire, Dunod, Paris 2001.
[39] Mathew, A. T., Numerical Analysis of Optimal Control Problems Governed by the Heat Equation. PhD Thesis, University of Oxford, (2016).
[40] Manuel Gonzales Burgos, Contrôlabilité des systèmes paraboliques, Ecole CIMPA-Kernitra(Maroc),2020.
[41] North, G. R., Cahalan, R. F., and Coakley Jr, J. A., Energy balance climate models." Reviews of Geophysics, 19(1), 1981, 91-121.
[42] O.Thual, Introduction aux méthodes spectrales, Institut national Polytechnique de Toulouse, 1996.
[43] Pironneau, O., Optimal Shape Design for Elliptic Systems. Springer, (2018).
[44] P.Joyal et A. Mercier. Analyse vectoriel. 1998.
[45] Ramanathan, V., The role of ocean–atmosphere interactions in the CO2 climate problem, Journal of the Atmospheric Sciences, 38(5), 1981, 918-930.
[46] Raymond, J.-P., and Thevenet, L., Boundary control and stabilization for parabolic equations. ESAIM: COCV, 2020.
[47] Robert A. Adams and John J. F. Fournier,*Sobolev Spaces*, Academic Press, 2003.
[48] Richmyer R.D. and Morton K.W. Difference methods for initial value Problems; Intersciences, Newyork 1967.
[49] SAMIE Dawaïdom, EDARH-BOSSOU Toyo Koffi, TCHARIE Kokou, *Long time solutions for a coupled parabolic and Hamilton-Jacobi equations*, Int. J. Adv. Appl. Math. and Mech. 9(2) (2021) 38– 45 (ISSN: 2347-2529).
[50] S. Candel, Mecanique des fluides, Dunod, 1995.
[51] Sellers, W. D., A global climatic model based on the energy balance of the Earth-atmosphere system, Journal of Applied Meteorology and Climatology, 8(3), 1969, 392-400.
[52] Tahirou Aboubacar Haboubacar, Djibo Moustapha and Saley Bisso, *Resolution and numerical simulation of a control problem of the heat equation*, International Journal of Numerical Methods and

Applications 23 (2023), 1-17.

[53] Tahirou Aboubacar Haboubacar, Djibo Moustapha and Saley Bisso, *Resolution and numerical simulation of a control problem of the heat equation*, International Journal of Numerical Methods and Applications 23 (2023), 1-17.

[54] Trefethen, L. N., Spectral Methods in MATLAB. Society for Industrial and Applied Mathematics, 2000.

[55] Trenberth, K. E., and Fasullo, J. T., Tracking Earth's energy: From El Niño to global warming, Surveys in Geophysics, 33(3-4), 2010, 413-426.

[56] Walter Rudin, Functional Analysis , McGraw-Hill, 1991.

[57] Y.Cherruault. Sur la convergence de la méthode d'Adomian, RAIRO. Recherche opérationnelle, tome 22, $n^o$3 1988.